Shell model Monte Carlo method in the *pn*-formalism and applications to the Zr and Mo isotopes

C. Özen[1] and D. J. Dean[2]
[1]*Department of Physics and Astronomy, University of Tennesee, Knoxville, Tennessee 37996, USA*
[2]*Physics Division, Oak Ridge National Laboratory, Oak Ridge, Tennessee 37831, USA*
(Received 5 August 2005; published 18 January 2006)

We report the development of a new shell model Monte Carlo algorithm, which uses the proton-neutron formalism. Shell model Monte Carlo methods, within the isospin formulation, have been succesfully used in large-scale shell model calculations. Motivation for this work is to extend the feasibility of these methods to shell model studies involving nonidentical proton and neutron valence spaces. We show the feasibility of the new approach with some test results. Finally, we use a realistic nucleon-nucleon interaction in the model space described by $(1p_{1/2}, 0g_{9/2})$ proton and $(1d_{5/2}, 2s_{1/2}, 1d_{3/2}, 0g_{7/2}, 0h_{11/2})$ neutron orbitals above the ^{88}Sr core to calculate ground-state energies, binding energies, $B(E2)$ strengths, and to study pairing properties of the even-even $^{90-104}$Zr and $^{92-106}$Mo isotope chains.

DOI: 10.1103/PhysRevC.73.014302 PACS number(s): 21.60.Ka

I. INTRODUCTION AND MOTIVATION

The shell model Monte Carlo (SMMC) method [1–3] was developed as an alternative to direct diagonalization in order to study low-energy nuclear properties. It was succesfully applied to nuclear problems in which large model spaces made diagonalization impractical. In the canonical SMMC approach, one calculates the thermal expectation values of observables of few-body operators by representing the imaginary-time many-body evolution operator as a superposition of one-body propagators in fluctuating auxiliary fields. Thus one recasts the Hamiltonian diagonalization problem as a stochastic integration problem.

In this paper, we report on the development of a SMMC approach in the *pn*-formalism. This implementation of SMMC enables one to treat shell model Hamiltonians that are not isospin invariant in the model space or for which different model spaces are used for protons and neutrons. In what follows, we use the abbreviated form SMMC*pn*, to distinguish the approach discussed here from the original one. We note that special features of the pairing-plus-quadrupole interaction enabled a special implementation of SMMC in nondegenerate proton and neutron model spaces for calculations in rare-earth nuclei [4,5]. The method presented in this work is general and may be used for realistic Hamiltonians as well those of a more schematic variety.

As a first novel application of the new implementation, we perform shell model calculations for the even-even $^{90-104}$Zr and $^{92-106}$Mo isotopic chains. Initial experimental studies [6] indicated that nuclei in this region have very large deformations and that the transition from spherical shapes to highly deformed shapes occurs abruptly: ^{96}Zr is rather spherical while $^{100-104}$Zr nuclei are well deformed with a quadrupole deformation parameter of $\beta_2 = 0.35$ [7]. Furthermore, the spherical-to-deformed transition is more abrupt in the Zr isotopes than in the nearby elements Mo, Ru and Pd. Generator-coordinate mean-field calculations in this region [8] are able to reproduce the shape transitions with particular Skyrme interactions. Furthermore, the region exhibits significant shape-coexistence phenomena [9,10].

The history of shell model applications in this mass region goes back to the 1960s with model spaces built on ^{88}Sr or ^{90}Zr cores [11–14]. Gloeckner [15] used an effective interaction built on a ^{88}Sr core with a model space consisting the orbitals π:$(1p_{1/2}, 0g_{9/2})$, ν:$(1d_{5/2}, 2s_{1/2})$. Other studies used larger model spaces [16–18] with varying effective interactions and truncation schemes. Holt *et al.* [19] derived a realistic effective interaction by using many-body perturbation techniques [20] in the model space π:$(1p_{1/2}, 0g_{9/2})$, ν:$(1d_{5/2}, 2s_{1/2}, 1d_{3/2}, 0g_{7/2}, 0h_{11/2})$. This effective interaction was based on the realistic nucleon-nucleon CD-Bonn potential [21], and shell model diagonalization calculations were carried out for the low-lying spectra of the Zr isotopes with neutron numbers from $N = 52$ to $N = 60$. Their results showed reasonable agreement with experimental spectra. In this paper, we use a slightly modified version of this realistic effective interaction to explore Zr and Mo nuclei through $N = 64$.

In Sec. II, we give an outline of the SMMC method with an emphasise on the differences in the SMMC*pn* implementation when compared with the isospin-conserving implementation. Then, in Subsec. III A, we demonstrate the utility of the new approach by a comparison of various numerical results we obtained by using the SMMC*pn* technique for a few *fp*-shell nuclei with those calculated by direct diagonalization and earlier SMMC studies. Calculations for the Zr and Mo isotopes, which are presented in Subsec. III B, were carried out in the same model space as that in Holt *et al.* [19], by use of a slightly modified interaction [22]. We show results for ground-state energies, binding energies, $B(E2)$ strengths, and BCS-like pairing correlations for the Zr and Mo isotope chains. We conclude with a perspective on this avenue of research.

II. FORMALISM

The SMMC method calculates expectation values of operators within a thermal ensemble of particles whose interactions are governed by the Hamiltonian $\hat{H}$ of the system. (A zero-temperature formalism also exists, but is not discussed

here.) The canonical expectation value of an operator $\hat{X}$ at a temperature T is given by

$$\langle \hat{X} \rangle = \frac{\mathrm{Tr}[\hat{U}\hat{X}]}{Z}, \tag{1}$$

where the partition function of the system is given by $Z(\beta) = \mathrm{Tr}\,\hat{U}$, $\beta = 1/kT$ is the inverse temperature, and the many-body evolution operator is $\hat{U} = e^{-\beta\hat{H}}$. The quantum-mechanical trace of an operator is defined as

$$\mathrm{Tr}\,\hat{X} = \sum_{\alpha} \langle \alpha | \hat{X} | \alpha \rangle, \tag{2}$$

where the sum runs over *all* many-body states in the Hilbert space. For nuclear calculations, the number of valence particles is usually limited, so that number projection becomes important. The original SMMC method preserved isospin within the same neutron and proton model spaces. In what follows, we discuss how to implement number projection when the isospin quantum number is broken. Note that, in the limit of $\beta \to \infty$, we may evaluate ground-state properties of the nuclear systems.

In the following, we discussion consider Hamiltonians that have at most two-body terms. Any such Hamiltonian can be cast into a quadratic form:

$$\hat{H} = \sum_{i} \epsilon_{\alpha} \hat{\rho}_{\alpha} + \frac{1}{2} \sum_{\alpha} \lambda_{\alpha} \hat{\rho}_{\alpha}^{2}, \tag{3}$$

where ε_α is the energy of single-particle level α and the operator $\hat{\rho}_\alpha$ is a a one-body density operator of the form $a^\dagger a$. Details are given in [1] on how to transform one-body operators with quantum numbers $\{n, l, j, j_z, t_z\}$ (where n is the principal quantum number, l is the orbital momentum, j is the total angular momentum and j_z is its projection, and $t_z = \pm 1$ for protons and neutrons) to the form shown in Eq. (3).

At the heart of the SMMC method lies the linearization of the imaginary-time many-body propagator. Since in general, $[\hat{\rho}_\alpha, \hat{\rho}_\beta] \neq 0$ we must split the interval β into N_t "time slices" of length $\Delta\beta \equiv \beta/N_t$. We apply the Hubbard-Stratonovich transformation [23,24] to the two-body evolution operator at each time slice. In compact notation, the partition function can be written as

$$\begin{aligned} Z &= \mathrm{Tr}\,\hat{U} = \mathrm{Tr}\, e^{-\beta\hat{H}} \longrightarrow \mathrm{Tr}[e^{-\Delta\beta\hat{H}}]^{N_t} \\ &\longrightarrow \int \mathfrak{D}[\sigma] G(\sigma) \mathrm{Tr}\,\hat{U}_\sigma, \end{aligned} \tag{4}$$

where the metric of the functional integral is

$$\mathcal{D}[\sigma] = \prod_{\alpha,n} \sqrt{\frac{\Delta\beta|V_\alpha|}{2\pi}} d\sigma_\alpha(\tau_n), \tag{5}$$

and the Gausian weight is given by

$$G_\sigma = e^{-\frac{1}{2}\Delta\beta \sum_{\alpha,n} |\lambda_\alpha| \sigma_\alpha^2(\tau_n)}. \tag{6}$$

The one-body evolution operator is written as

$$\hat{U}_\sigma = \prod_{n=1}^{N_t} e^{-\Delta\beta \hat{h}_\sigma(\tau_n)} \equiv \mathcal{T} e^{-\int_0^\beta d\tau \hat{h}_\sigma(\tau)}, \tag{7}$$

where we note the dependence on the auxiliary fields $\sigma(\tau_n)$. This-time ordered product means that this formalism yields a path integral in the fields σ. The linearized one-body Hamiltonian for the time slice τ_n is given by

$$\hat{h}_\sigma(\tau_n) = \sum_i \varepsilon_\alpha \hat{\rho}_\alpha + \sum_{\alpha n} s_\alpha \lambda_\alpha \sigma_\alpha(\tau_n) \hat{\rho}_\alpha, \tag{8}$$

with $s = \pm 1$, if $\lambda > 0$ or $s = \pm i$ if $\lambda < 0$. Note that, because the various $\hat{\rho}_\alpha$ need not commute, Eq. (7) is accurate only through order $\Delta\beta$ and that the representation of $e^{-\Delta\beta\hat{h}}$ must be accurate through order $\Delta\beta^2$ to achieve that accuracy.

The thermal expectation values can be expressed as the ratio of path integrals in fluctuating auxiliary fields,

$$\langle \hat{O} \rangle = \frac{\mathrm{Tr}[\hat{O}e^{-\beta\hat{H}}]}{\mathrm{Tr}[e^{-\beta\hat{H}}]} = \frac{\int \mathcal{D}[\sigma] G_\sigma \langle \hat{O} \rangle_\sigma \xi_\sigma}{\int \mathcal{D}[\sigma] G_\sigma \xi_\sigma}, \tag{9}$$

where the following definitions are used:

$$\xi_\sigma = \mathrm{Tr}\,\hat{U}_\sigma, \quad \langle \hat{O} \rangle_\sigma = \frac{\mathrm{Tr}\,[\hat{O}\hat{U}_\sigma]}{\mathrm{Tr}\,\hat{U}_\sigma}. \tag{10}$$

To use the Monte Carlo sampling methods, of Metropolis *et al.* [25], we need to define a positive-definite weight function,

$$W_\sigma = G_\sigma |\xi_\sigma|, \tag{11}$$

so Eq. (9) can now be rewritten as

$$\langle \hat{O} \rangle = \frac{\int \mathcal{D}[\sigma] W_\sigma \langle \hat{O} \rangle_\sigma \Phi_\sigma}{\int \mathcal{D}[\sigma] W_\sigma \Phi_\sigma} \equiv \frac{\langle \langle \hat{O} \rangle_\sigma \Phi_\sigma \rangle_W}{\langle \Phi_\sigma \rangle_W}, \tag{12}$$

where

$$\Phi_\sigma = \frac{\xi_\sigma}{|\xi_\sigma|} \tag{13}$$

is the sign of the partition function.

The description above shows how one may transform the shell model into a problem of quadrature integration. Objects, ξ_σ and $\langle \hat{X} \rangle_\sigma$, in the integrands are of one-body nature and are represented by $N_s \times N_s$ dimensional matrices, where N_s is the number of the single-particle levels in the valence space. The path integrals in the auxiliary fields are evaluated by performing a Metropolis random walk in the field space. Thermodynamic expectation values are given as the ratio of two multidimensional integrals over the auxiliary fields. The dimension D of these integrals is of the order of $N_s^2 N_t$, which can exceed 10^5 for the problems of interest.

Note that the Monte Carlo sign problem enters calculations when any of the λ_α matrix elements is positive. Realistic shell-model interactions always have such terms; a special case is the pairing-plus-quadrupole Hamiltonian that has no sign problems.

If the proton and neutron valence spaces are identical and the Hamiltonian $\hat{H}$ is isospin symmetric, then the Hamiltonian can be cast into a quadratic form that respects this symmetry explicitly. In that case, it is possible to form linear combinations of density operators that separately conserve the neutron and proton numbers. In the isospin formulation (as done in the original shell model Monte Carlo studies) proton and neutron wave functions can be represented by separate

Slater determinants, and the ensuing one-body propagator factors into two propagators as well, one for protons and another for neutrons. The canonical traces are then calculated by application of the number-projection operator to obtain the desired proton and neutron numbers. In contrast, we apply the SMMC method to Hamiltonians that are not necessarily isospin invariant or for which proton and neutron valence spaces are different. A relaxation of the isospin symmetry in the quadratic forms becomes essential for employing the SMMC method in such cases. In the *pn*-formalism, proton and neutron valence spaces are no longer distinguished from each other; instead, we consider a single-valence space containing both proton and neutron orbitals. In this way, the density operators in the one-body Hamiltonian $h(\sigma)$ inevitably mix protons and neutrons, and as a consequence their respective expectation values will fluctuate from sample to sample. In principle, this mixing can be averted by use of a suitable combination of direct and exchange formulations of the decomposition [3]; however, because the choice of decomposition is directly related to the the fluctuations of the Monte Carlo sign and thus the stability of the calculation, it may be desirable to have a method to deal with the mixing, that is independent of the decomposition approach. In this paper, we chose to use a direct decomposition only, and to explore, for the first time, how the SMMC formalism could be extended to incorporate number and T_z projections in the case in which the one-body densities include proton-neutron terms. The canonical trace is then retrieved by use of projection operators to fix the total number of particles A and the z component of the total isospin T_z. This implementation represents the major difference between the original SMMC and the SMMC*pn* techniques.

Projection operators for fixed A and T_z are given by

$$\hat{P}_A = \int_0^{2\pi} \frac{d\phi}{2\pi} e^{-i\phi A} e^{i\phi \hat{N}} \tag{14a}$$

and

$$\hat{P}_{T_z} = \int_0^{2\pi} \frac{d\theta}{2\pi} e^{-i\theta T_z} e^{i\theta \hat{T}_z}, \tag{14b}$$

respectively. In the discrete Fourier representation, we make the substitution

$$\int_0^{2\pi} \frac{d\phi}{2\pi} \int_0^{2\pi} \frac{d\theta}{2\pi} \longrightarrow \frac{1}{N_s(N_{T_z}+1)} \sum_{m=1}^{N_s} \sum_{n=0}^{N_{T_z}}, \tag{15}$$

where the quadrature points are given by $\phi_m = 2\pi m/N_s$ and $\theta_n = 2\pi n/(N_{T_z}+1)$, and N_{T_z} is the number of values T_z can take. As an example, the canonical trace of the one-body propagator $\hat{U}_\sigma$ can be obtained by acting with both projection operators on the grand-canonical trace, $\mathrm{Tr}\,\hat{U}_\sigma = \det(1+\mathbf{U}_\sigma)$:

$$\begin{aligned} \mathrm{Tr}_{A,T_z}\hat{U}_\sigma &= \frac{1}{N_s(N_{T_z}+1)} \sum_{m,n} e^{-i\phi A} e^{-i\theta T_z} \mathrm{Tr}\, e^{i\phi\hat{N}} e^{i\theta\hat{T}_z} \hat{U}_\sigma \\ &= \frac{1}{N_s(N_{T_z}+1)} \sum_{m,n} e^{-i\phi A} e^{-i\theta T_z} \det(1 + e^{i\phi} e^{i\theta \mathbf{T_z}} \mathbf{U}_\sigma), \end{aligned} \tag{16}$$

where the boldface symbols are used for the matrix representation of the operators; for example,

$$\mathbf{T_z} = \frac{1}{2} \left(\begin{array}{c|c} -\mathbf{1} & \mathbf{0} \\ \hline \mathbf{0} & \mathbf{1} \end{array} \right). \tag{17}$$

A typical difficulty in the SMMC applications is due to a sign problem arising from the repulsive part of the realistic interactions. In the case of realistic interactions, a straightforward application of Eq. (11) to obtain a positive-definite weight will introduce a highly fluctuating weight function. This will give rise to expectation values with very large fluctuations. To avoid this situation, we adopt a practical solution [26] to the sign problem by breaking the two-body interaction into "good" (without a sign problem) and "bad" (with a sign problem) parts: $H = H_G + H_B$. Using a parameter g, we then construct a new family of Hamiltonians $H(g) = H_G + gH_B$ that are free of the sign problem for nonpositive values of g. The SMMC observables are evaluated for a number of different g values in the interval $-1 \leqslant g \leqslant 0$, and the physical values are thus retrieved by extrapolation to $g = 1$. We use polynomial extrapolations and choose the minimum order that gives $\chi \approx 1$. In our calculations, most of the extrapolations are linear or quadratic. In the extrapolation of $\langle H \rangle$, variational principle imposes a vanishing derivative at the physical value $g = 1$. A cubic extrapolation in this case typically gives the best results.

We note that in the SMMC*pn* formalism the sign problem will occur, even when one has a good interaction, for all nuclei for which either the proton or the neutron number (or both) is odd. This contrasts to the original SMMC implementation in which all $N = Z$ nuclei have no sign problem when a good interaction is used.

Another problem encountered in applying the SMMC methods concerns efficiency of the Metropolis algorithm in generating uncorrelated field configurations. Rather than sample continuous fields, for which decorrelated samples are obtained after only very many (of the order of 200) Metropolis steps, we approximate the continuous integral over each $\sigma_\alpha(\tau_n)$ by a discrete sum derived from a Gaussian quadrature [4]. In particular, the relation

$$e^{\Delta\beta\lambda\hat{\rho}^2/2} \approx \int_{-\infty}^{\infty} d\sigma f(\sigma) e^{\Delta\beta\lambda\sigma\hat{\rho}} \tag{18}$$

is satisfied through terms in $(\Delta\beta)^2$ if

$$f(\sigma) = \tfrac{1}{6}\left[\delta(\sigma-\sigma_0) + \delta(\sigma+\sigma_0) + 4\delta(\sigma)\right], \tag{19}$$

where $\{\sigma_0 = (3/\lambda\Delta\beta)^{1/2}\}$. In the SMMC*pn* algorithm we find that samples are well decorrelated after only a few (typically fewer than 10) Metropolis steps using these descretized fields.

We describe in the following section our initial results we obtained by using the SMMC*pn* method.

TABLE I. Comparison of the ground-state energies (in MeV), as calculated by SMMC*pn* and the ANTOINE results. A quadrupole-plus-pairing interaction is used.

Nucleus	E (ANTOINE)	E (SMMC*pn*)
^{24}Mg	-39.28	-38.68 ± 0.27
^{26}Mg	-43.58	-42.75 ± 0.70
^{22}Ne	-30.23	-29.53 ± 0.41
^{28}Si	-49.25	-48.80 ± 0.37

III. RESULTS

A. Comparisons with direct diagonalization and previous SMMC calculations

In this section, we present a number of test cases that validate the SMMC*pn* approach. For this purpose, we first carried out calculations on a few *sd*-shell nuclei, using a quadrupole-plus-pairing interaction that is free of the sign-problem. This interaction can be written as

$$\hat{V} = -\chi \hat{Q} \cdot \hat{Q} - g \hat{P}^{(0,1)\dagger} \cdot \tilde{\hat{P}}^{(0,1)}, \tag{20}$$

where

$$\hat{Q} = \frac{1}{\sqrt{5}} \sum_{ab} \langle j_a | \left| \frac{dV_{\rm WS}}{dr} Y_2 \right| | j_b \rangle \left[a^\dagger_{j_a} \otimes \tilde{a}_{j_b} \right]^{J=1,T=0} \tag{21}$$

and

$$\hat{P}^{(0,1)\dagger} = \sum_a \left[a^\dagger_{j_a} \otimes a^\dagger_{j_a} \right]^{J=0,T=1}. \tag{22}$$

The strength of the interaction terms were chosen as $\chi = 0.0260$ MeV^{-1} fm^2 and $g = 0.212$ MeV. We adopted the standard Universal SD (USD) shell model interaction [27] single-particle energies. The term $V_{\rm WS}$ in the equation above is the central part of a Woods-Saxon potential with parameters given in [28]. The SMMC*pn* calculations were performed at $\beta = 2$ MeV^{-1} with $N_t = 128$ time slices ($\Delta\beta = 1/64$ MeV^{-1}), and each calculation involved 2500–3000 uncorrelated samples. Note that typical isospin-conserving SMMC calculations require only $\Delta\beta = 1/32$ MeV^{-1} for similar convergence. A comparison of our results with the direct diagonalization values (which we obtained by running the ANTOINE [29] code) is given in Table I. Results are compatible within the internal heating energy and statistical errors of the thermal SMMC calculations.

We also tested the feasibility of the new implementation with the utilization of the extrapolation method described above. For this purpose, a few *fp*-shell nuclei were chosen and the modified Kuo-Brown KB3 residual interaction [30] was used. We calculated the ground-state energies, total $B(M1)$, $B(E2)$, and the Gamow-Teller strengths of the nuclei and compared our results with those obtained by exact diagonalization [31] and those obtained by the isospin SMMC [32]. The SMMC*pn* calculations were performed at $\beta = 2$ MeV^{-1} with $\Delta\beta = 1/64$ MeV^{-1}, and each calculation at each of six values of the extrapolation parameter g involved 8000–9000 uncorrelated samples. We used a quadratic extrapolation for the total $B(M1)$ and B(GT+) strengths, while for the total $B(E2)$ strengths a linear extrapolation was more reasonable. The ground-state energies employed cubic polynomials subject to the constraint $d\langle H \rangle / dg|_{g=1} = 0$ because of a variational principle that $\langle H \rangle$ obeys. In all the cases, the errors were conservatively adopted from a quadratic extrapolation.

In Table II, ground-state energies and $B(E2)$ strengths are tabulated. In all cases, the energies agree strikingly well within error bars that are reasonable with the internal excitation energy of a few hundred kilo-electron-volts because of the finite-temperature calculations. The $B(E2)$ strength is given by

$$B(E2) = \langle (e_p \hat{Q}_p + e_n \hat{Q}_n)^2 \rangle, \tag{23}$$

where the quadrupole operator is defined as $\hat{Q}_{p(n)} = \sum_i r_i^2 Y_2(\theta_i, \phi_i)$. The effective charges were chosen to be $e_p = 1.35$ and $e_n = 0.35$, and the oscillator strength is given by $b = 1.01 A^{1/6}$. $B(E2)$ values are also nicely reproduced in general, while in the case of ^{48}Cr, the exact result is underestimated by $\approx$25%.

Table III shows a comparison of results for the $B(M1)$ and B(GT+) strengths. The $B(M1)$ strength is defined by

$$B(M1) = \left\langle \left(\sum_i \mu_N \{ g_l \vec{l} + g_s \vec{s} \} \right)^2 \right\rangle, \tag{24}$$

where μ_N is the nuclear magneton. We used the bare g factors for angular momentum and spin ($g_l = 1$ and $g_s = 5.586$ for protons and $g_l = 0$ and $g_s = -3.826$ for neutrons). The Gamow-Teller strength is defined by

$$B(\mathrm{GT}+) = \langle \mathrm{G}_\mp \mathrm{G}_\pm \rangle, \tag{25}$$

where the unquenched Gamow-Teller operator is written as $G_\pm = \sum_i \vec{\sigma} t_\pm$. Both $B(M1)$ and B(GT+) results agree well with those obtained by direct diagonalization. Last, as in the case of isospin SMMC calculations, our calculations satisfy the Ikeda sum rule $B(\mathrm{GT}-) - \mathrm{B(GT+)} = 3(\mathrm{N} - \mathrm{Z})$ exactly.

TABLE II. Comparison of exact diagonalization, SMMC*pn*, and isospin SMMC results for valence space energies (in MeV) and $B(E2)$ strengths (in e^2 fm^4). A typical error bar for energies is ± 0.6 MeV for SMMC*pn* and ± 0.4 MeV for isospin SMMC calculations.

Nucleus	E exact	E SMMC (*pn*)	E SMMC (iso)	$\sum B(E2)$ exact	$\sum B(E2)$ SMMC (*pn*)	$\sum B(E2)$ SMMC (iso)
^{48}Ti	-24.6	-24.4	-23.9	476	459 ± 33	455 ± 25
^{48}Cr	-32.9	-32.6	-32.3	978	745 ± 40	945 ± 45
^{56}Fe	-66.4	-66.0	-65.8	1019	913 ± 55	990 ± 6
^{64}Zn	-106.3	-106.5	-104.8	1157	1116 ± 81	1225 ± 65

TABLE III. Comparison of exact diagonalization, SMMC*pn*, and isospin SMMC results for $B(M1)$ (in μ_N) and Gamow-Teller strengths.

Nucleus	$\sum B(M1)$ exact	$\sum B(M1)$ SMMC(*pn*)	$\sum B(M1)$ SMMC (iso)	$\sum B(\mathrm{GT}+)$ exact	$\sum B(\mathrm{GT}+)$ SMMC(*pn*)	$\sum B(\mathrm{GT}+)$ SMMC (iso)
^{48}Ti	10.6	10.4 ± 4	10.2 ± 1.2	1.26	0.89 ± 0.36	1.13 ± 0.18
^{48}Cr	12.0	12.5 ± 4.4	13.8 ± 1.7	4.13	4.35 ± 0.44	4.37 ± 0.35
^{56}Fe	19.4	22.6 ± 6.4	20.4 ± 3.0	4.69	4.02 ± 0.55	3.99 ± 0.27
^{64}Zn	21.6	22.8 ± 1.2	23.6 ± 2.2	5.54	5.66 ± 0.7	4.13 ± 0.34

B. Applications to Zr and Mo isotopes

Calculations for the Zr and Mo isotopes were carried out in the same valence space as in Holt *et al*. [19], which is built on the ^{88}Sr core, but we employed a slightly modified interaction that had been previously tested for nuclei with small numbers of valence particles in this region [22]. The model space and single-particle energies that were used in the calculations are given in Table IV ([19] and references therein). We performed calculations at $\beta = 2$ MeV^{-1} using $N_t = 128$ time intervals with 8500–9500 uncorrelated samples for each extrapolation parameter g.

1. Ground-state energies

Shown in Fig. 1 is the comparison of the expectation value of energy $\langle \hat{H} \rangle$. Filled circles that are connected with dashed lines represent exact diagonalization results obtained by Juodagalvis [33], and in both the Zr and Mo cases, the agreement of the SMMC*pn* values is remarkable. Only for ^{94}Zr do the error bars of the SMMC*pn* result miss the exact value slightly. This represents the full test of the SMMC*pn* approach.

2. Binding energies

The ground-state energies shown in Fig. 1 correspond to the contribution to the nuclear binding energy of the interaction of the valence particles among themselves.

In Fig. 2, we plot calculated and experimental values of binding energies with respect to the ^{88}Sr core. We used the following formulas to obtain our binding energies (BE):

$$\begin{aligned} \mathrm{BE}(^{90+n}\mathrm{Zr}) = {} & \mathrm{BE}(^{90+n}\mathrm{Zr}) - \mathrm{BE}(^{88}\mathrm{Sr}) \\ & - n[\mathrm{BE}(^{89}\mathrm{Sr}) - \mathrm{BE}(^{88}\mathrm{Sr})] \\ & - 2[\mathrm{BE}(^{89}\mathrm{Y}) - \mathrm{BE}(^{88}\mathrm{Sr})], \end{aligned} \tag{26}$$

TABLE IV. The model space and single-particle energies used in these calculations. Note also that the effective charges for protons and neutrons are $e_P = 1.8e$ and $e_n = 1.5e$. The oscillator parameter is $b = 2.25$ fm.

Protons		Neutrons	
Orbital	Energy (MeV)	Orbital	Energy (MeV)
$0g_{9/2}$	0.90	$0h_{11/2}$	3.50
$1p_{1/2}$	0.00	$0g_{7/2}$	2.63
		$1d_{3/2}$	2.23
		$2s_{1/2}$	1.26
		$1d_{5/2}$	0.00

$$\begin{aligned} \mathrm{BE}(^{92+n}\mathrm{Mo}) = {} & \mathrm{BE}(^{92+n}\mathrm{Mo}) - \mathrm{BE}(^{88}\mathrm{Sr}) \\ & - n[\mathrm{BE}(^{89}\mathrm{Sr}) - \mathrm{BE}(^{88}\mathrm{Sr})] \\ & - 4[\mathrm{BE}(^{89}\mathrm{Y}) - \mathrm{BE}(^{88}\mathrm{Sr})]. \end{aligned} \tag{27}$$

An inspection of the resulting relative binding energies shows that the calculated values in Fig. 2 (shown by asterisks) deviate from the experimental values (shown by filled circles), which display a parabolic behavior. This situation is common among calculations made with realistic interactions derived from *NN* scattering data [34]. It may be related to the absence of real three-body forces in the construction of the effective two-body interactions [35]. It is known that a given Hamiltonian can always be separated in the form $\hat{H} = \hat{H}_m + \hat{H}_M$, where $\hat{H}_m$ is the monopole part, while the multipole $\hat{H}_M$ contains all other terms [36]. $\hat{H}_M$ given by realistic *NN* interactions takes proper account of the configuration mixing; however, the monopole part $\hat{H}_m$ fails to produce the correct unperturbed energies. It is possible to change the averages of the so-called centroid matrix elements to fix this failure without affecting the spectrosopy to produce the correct binding energies [37]. However, a rigorous treatment of the global monopole corrections would

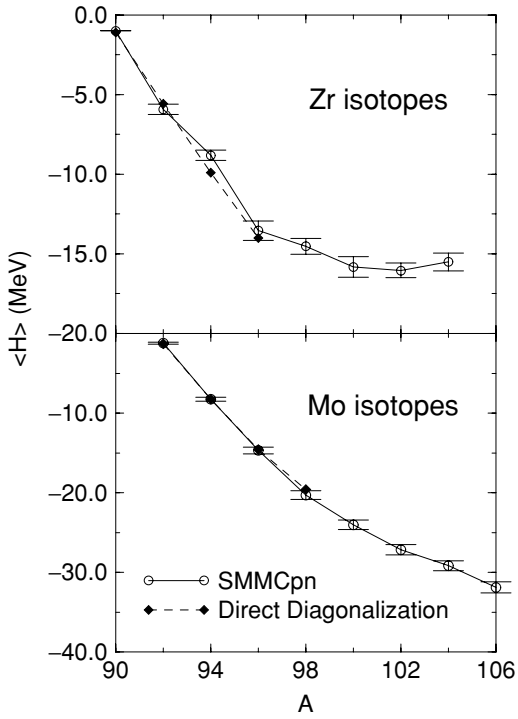

FIG. 1. Ground-state energies of Zr and Mo isotopes. Results from direct diagonalization avaliable for lighter isotopes also shown.

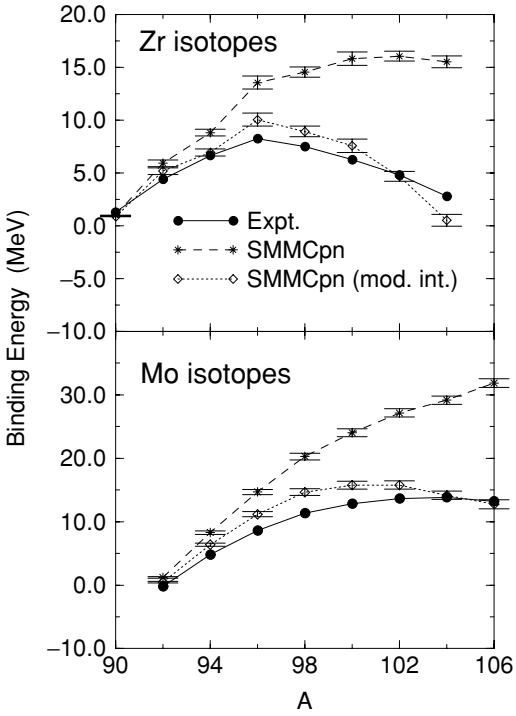

FIG. 2. Binding energies of the Zr and Mo isotopes.

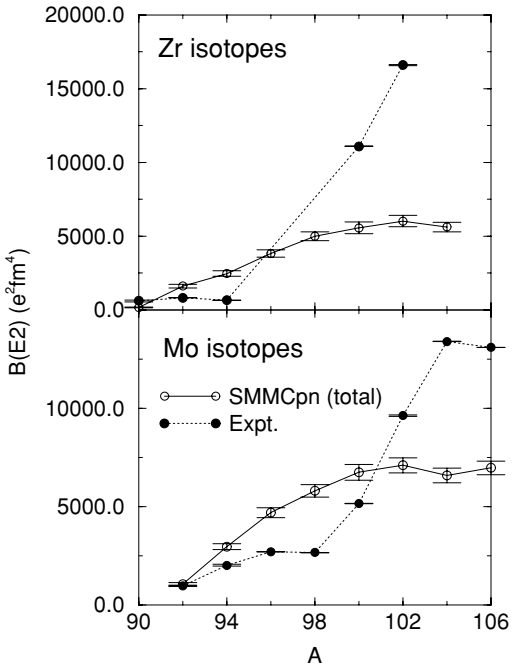

FIG. 3. Total $B(E2)$ strengths from the ground state for Zr and Mo isotopes. Experimental results are for $0_1^+ \rightarrow 2_1^+$.

deserve a detailed study and thus goes beyond the scope of the current work. Instead, to give some substance to how a monopole correction may work, we add an overall constant to the diagonal interaction elements so that the modified matrix elements are given by

$$V_J^{\mathrm{mod}}(ab, ab) = V_J(ab, ab) + W\frac{n(n-1)}{2}, \qquad (28)$$

where n is the number of valence particles. We have adopted $W = -125$ keV to reproduce the binding energy of ^{102}Zr. We plot the effect of this rather naive correction in Fig. 2, in which modified results, represented by diamonds, show much better agreement for both chains of isotopes.

3. $B(E2)$ strengths

Since the 2_1^+ state is expected to absorb most of the total $B(E2)$ strength, the latter can be used as a measure of the 0_1^+–2_1^+ spacing, which should reflect a strong change with the shape transitions. Shown in Fig. 3 are the calculated total $B(E2)$ strengths (open circles) and available experimental [38] $0_1^+ \rightarrow 2_1^+$ values (filled circles). Despite the fact that the calculated total strengths increase as expected in both isotope chains with the addition of neutrons, their numerical values fall somewhat below the experimental $B(E2; 0_1^+ \rightarrow 2_1^+)$ values on the heavier side of the isotope chains. We also investigated whether this situation would improve by lowering the $Oh_{11/2}$ single-particle energy since it has been suggested [39] that the $Oh_{11/2}$ significantly contributes to deformation in this region. We found that even a substantial lowering of the single-particle energy to 2.0 MeV only increased the $B(E2)$ in Zr by approximately 5%. This inability to obtain a very large $B(E2)$ is quite possibly due to correlations that are absent because of our choice of model space. We will investigate this further in future work.

4. Pairing correlations

Pairing correlations among like nucleons is known to be important for the ground-state properties of the even-even nuclei [40]. These correlations should become quenched along the Zr and Mo isotope chains as the transition from spherical to well-deformed shapes becomes more pronounced. Similar effects were recently investigated in $N = 40$ isotones [41]. We have investigated the pairing content of the ground states of the nuclei of interest by using a BCS-like pair operator that is defined for neutrons as

$$\hat{\Delta}_\nu^\dagger = \sum_{jm>0} \nu_{jm}^\dagger \nu_{j\bar{m}}^\dagger, \qquad (29)$$

where the sum is over all orbitals with $m > 0$ and $\nu_{j\bar{m}}^\dagger = (-1)^{j+m}\nu_{j-m}^\dagger$ is the time-reversed operator. Hence the expectation value of the pairing fields is $\langle \hat{\Delta}_\nu^\dagger \hat{\Delta}_\nu \rangle$. This quantity for an uncorrelated Fermi gas is given by

$$\langle \hat{\Delta}^\dagger \hat{\Delta} \rangle = \sum_j \frac{n_j^2}{2(2j+1)}, \qquad (30)$$

where $n_j = \langle \nu_{jm}^\dagger \nu_{jm} \rangle$ are the neutron occupation numbers. Any excess over the Fermi gas value therefore indicates pairing correlations in the ground state. Our results, which are plotted in Fig. 4, confirm a suppression of these correlations, as the contribution of the added neutrons to the pairing gradually decreases and the correlations become noticeably quenched beyond ^{96}Zr and ^{100}Mo.

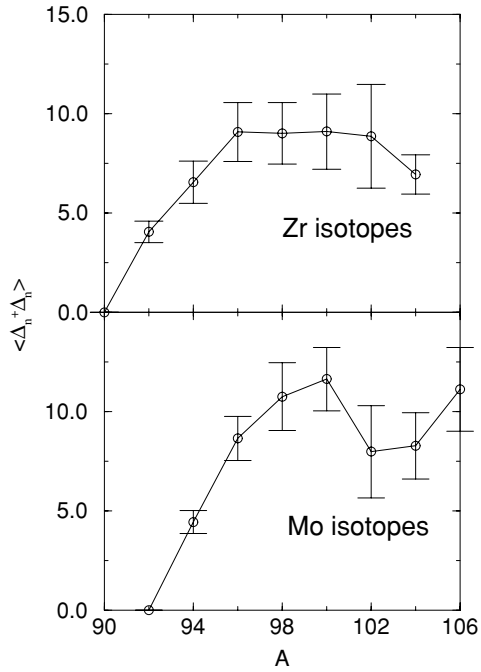

FIG. 4. Pairing correlations of Zr and Mo isotopes.

In addition, the occupation numbers of various orbitals are plotted in Fig. 5, demonstrating that additional neutrons are distributed into the available orbitals rather uniformly, while protons tend to migrate from the $0g_{9/2}$ to the $1p_{1/2}$ orbital. In the case of Mo isotopes, the spurious effect of exceeding the maximum-allowed occupancy for the $1p_{1/2}$ orbital is a result of the extrapolation scheme that was used and is indicative that

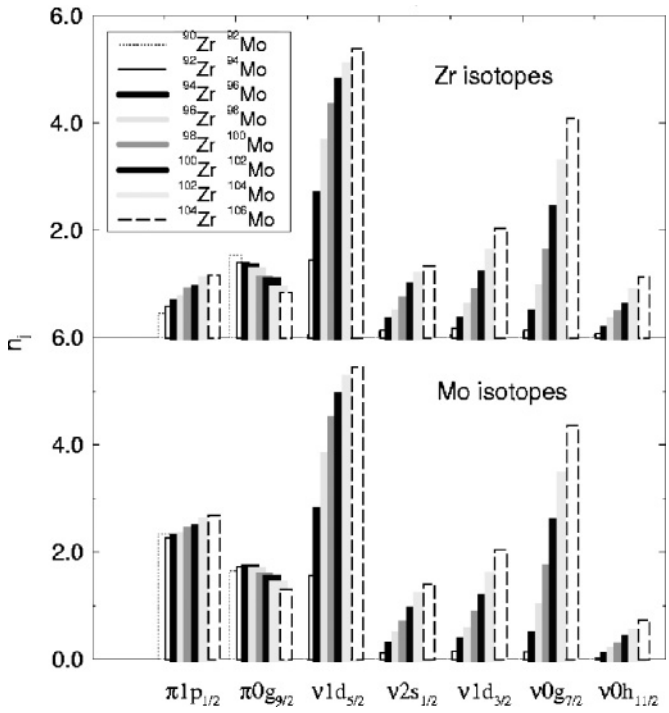

FIG. 5. Orbital occupation numbers.

the relative error bars on the occupation data after extrapolation are approximately 15% of the value of the occupation number. Note that the deformation driving $0h_{11/2}$ remains only slightly occupied.

IV. CONCLUSION AND PERSPECTIVES

We have introduced a new approach for the implementation of the SMMC method to perform shell model calculations by using nonidentical proton and neutron valence spaces. General features of the SMMC method were reviewed. Differences between the isospin and the *pn*-formalisms have been pointed out; in particular, the T_z projection has been described in detail.

The results of the SMMC*pn* approach have been validated in the *sd*-shell by a "good"-signed schematic interaction and in the *fp*-shell by the realistic KB3 interaction. In the latter case, we dealt with the sign problem by using an extrapolation method.

As the first novel application of the SMMC*pn* approach, we performed a set of calculations for the even-even $^{90-104}$Zr and $^{92-106}$Mo isotopes, using a realistic effective interaction in the valence space described by (π:$1p_{1/2}$, $0g_{9/2}$) and (ν: $1d_{5/2}$, $2s_{1/2}$, $1d_{3/2}$, $0g_{7/2}$, $0h_{11/2}$) orbitals.

A comparison of the ground-state energies of the first few nuclei in both isotope chains showed excellent agreement with the exact diagonalization results and provided a definitive test of our algorithm and the SMMC*pn* method. We then studied the transitional nature of the isotopes by using the $B(E2)$ strength as a gross measure of the 0_1^+–2_1^+ separation. Along both isotope chains, we obtained an enhancement in the $B(E2)$ strengths as a function of the added neutrons, accompanied by a quenching in the neutron-pairing correlations. In spite of this qualitative reproduction of the onset of deformations, clearly further research is needed for a qualitative result in the heavier Zr and Mo nuclei. A comparison with the experimental data suggests that this situation may be a shortcoming that is due to the degrees of freedom that are absent in the chosen valence space. We will investigate this further in following work.

Apart from future applications involving realistic effective interactions, use of schematic interactions in SMMC*pn* applications should be an interesting direction of research. Such interactions have been commonly used to calculate realistic estimates of collective properties and level densities; the latter is an important ingredient in the prediction of nuclear reaction rates in astrophysics. Parity dependence of these densities may play a crucial role in the nucleosynthesis. We believe that SMMC*pn* will prove to be a useful computational tool in this regard.

ACKNOWLEDGMENTS

We acknowledge useful discussions with M. Hjorth-Jensen. Supported by the U.S. Department of Energy under contract nos. DE-FG02-96ER40963 (University of Tennessee), DE-AC05-00OR22725 with UT-Battelle, LLC (Oak Ridge National Laboratory).

[1] S. E. Koonin, D. J. Dean, and K. Langanke, Phys. Rep. **278**, 1 (1997).
[2] S. E. Koonin, D. J. Dean, and K. Langanke, Annu. Rev. Nucl. Part. Sci. **47**, 463 (1997).
[3] G. H. Lang, C. W. Johnson, S. E. Koonin, and W. E. Ormand, Phys. Rev. C **48**, 1518 (1993).
[4] D. J. Dean, S. E. Koonin, G. H. Lang, W. E. Ormand, and P. B. Radha, Phys. Lett. **B317**, 275 (1993).
[5] J. A. White, S. E. Koonin, and D. J. Dean, Phys. Rev. C **61**, 034303 (2000).
[6] E. Cheifetz, R. C. Jared, S. G. Thompson, and J. B. Wilhelmy, Phys. Rev. Lett. **25**, 38 (1970).
[7] M. A. C. Hotchkis, J. L. Durell, J. B. Fitzgerald, A. S. Mowbray, W. R. Phillips, I. Ahmad, M. P. Carpenter, R. V. Janssens, T. L. Khoo, E. F. Moore, L. R. Morss, P. Benet, and D. Ye, Phys. Rev. Lett. **64**, 3123 (1990).
[8] J. Skalski, P.-H. Heenen, and P. Bonche, Nucl. Phys. **A559**, 221 (1993).
[9] P.-G. Reinhard, D. J. Dean, W. Nazarewicz, J. Dobaczewski, J. A. Maruhn, and M. R. Strayer, Phys. Rev. C **60**, 014316 (1999).
[10] J. L. Wood, K. Heyde, W. Nazarewicz, M. Huyse, and P. van Duppen, Phys. Rep. **215**, 101 (1992).
[11] I. Talmi and I. Unna, Nucl. Phys. **19**, 225 (1960).
[12] N. Auerbach and I. Talmi, Nucl. Phys. **64**, 458 (1965).
[13] J. Vervier, Nucl. Phys. **75**, 17 (1966).
[14] S. Cohen, R. D. Lawson, M. H. Macfarlane, and M. Soda, Phys. Lett. **10**, 195 (1964).
[15] D. H. Gloeckner, Nucl. Phys. **A253**, 301 (1975).
[16] S. S. Ipson, K. C. McLean, W. Booth, J. G. B. Haigh, and R. N. Glover, Nucl. Phys. **A253**, 301 (1975).
[17] P. Halse, J. Phys. G **19**, 1859 (1993).
[18] C. H. Zhang, S.-J. Wang, and J.-N. Gu, Phys. Rev. C **60**, 054316 (1999).
[19] A. Holt, T. Engeland, M. Hjorth-Jensen, and E. Osnes, Phys. Rev. C **61**, 064318 (2000).
[20] M. Hjorth-Jensen, T. T. S. Kuo, and E. Osnes, Phys. Rep. **261**, 125 (1995).
[21] R. Machleidt, F. Sammarruca, and Y. Song, Phys. Rev. C **53**, R1483 (1996).
[22] A. Juodagalvis and D. J. Dean, Phys. Rev. C **72**, 024306 (2005).
[23] J. Hubbard, Phys. Lett. **3**, 77 (1959).
[24] R. D. Stratonovich, Dokl. Akad. Nauk., SSSR **115**, 1907 (1957) [transl: Soviet Phys. Kokl. **2**, 416 (1958)].
[25] N. Metropolis, A. Rosenbluth, M. Rosenbluth, A. Teller, and E. Teller, J. Chem. Phys. **21**, 1087 (1953).
[26] Y. Alhassid, D. J. Dean, S. E. Koonin, G. Lang, and W. E. Ormand, Phys. Rev. Lett. **72**, 613 (1994).
[27] B. H. Wildenthal, Prog. Part. Nucl. Phys. **11**, 5 (1984).
[28] A. Bohr and B. R. Mottelson, *Nuclear Structure* (Benjamin, New York, 1969), Vol. 1.
[29] E. Caurier, computer code ANTOINE (Centrede Recherche Nucleaires, Strasbourg, France, 1989).
[30] A. Poves and A. P. Zuker, Phys. Rep. **70**, 235 (1981).
[31] E. Caurier, G. Martinez-Pinedo, F. Nowacki, A. Poves, J. Retamosa, and A. P. Zuker, Phys. Rev. C **59**, 2033 (1999).
[32] K. Langanke, D. J. Dean, P. B. Radha, Y. Alhassid, and S. E. Koonin, Phys. Rev. C **52**, 718 (1995).
[33] A. Juodagalvis (private communication).
[34] A. Holt, T. Engeland, M. Hjorth-Jensen, and E. Osnes, Nucl. Phys. **A634**, 41 (1998).
[35] A. P. Zuker, Phys. Rev. Lett. **90**, 042502 (2003).
[36] A. Abzouzi, E. Caurier, and A. P. Zuker, Phys. Rev. Lett. **66**, 1134 (1991).
[37] J. Duflo and A. P. Zuker, Phys. Rev. C **59**, R2347 (1999).
[38] C. W. Raman, S. Nestor Jr., and P. Tikkanen, At. Data Nucl. Data Tables **78**, 1 (2001).
[39] W. Nazarewicz, in *Contemporary Topics in Nuclear Structure Physics*, edited by R. F. Casten, A. Frank, M. Moshinsky, and S. Pittel (World Scientific, Singapore, 1988), p. 467.
[40] D. J. Dean and M. Hjorth-Jensen, Rev. Mod. Phys. **75**, 607 (2003).
[41] K. Langanke, D. J. Dean, and W. Nazarewicz, Nucl. Phys. **A757**, 360 (2005).